# Charge transfer and ionization involving Argon ions and neutral Hydrogen

**L. F. Errea, Clara Illescas, L. Méndez, B. Pons†, A. Riera and J. Suárez**

Laboratorio Asociado al CIEMAT de Física Atómica y Molecular en Plasmas de Fusión,
Departamento de Química C-IX, Universidad Autónoma, 28049 Madrid, Spain
† Centre Lasers Intenses et Applications, UMR 5107 du CNRS,
Université de Bordeaux-I, 351 Cours de la Libération, 33405 Talence, France

**Abstract.**

We present Classical Trajectory Monte Carlo (CTMC) calculations of total and partial cross sections for capture and ionization in $Ar^{18+}$, $Ar^{17+}$, $Ar^{16+}$ + H(1$s$) collisions in the 30 - 300 keV/amu impact energy range. We specially focus on capture into high-lying states of the projectile, which are of paramount importance for diagnostics of fusion plasmas involving $Ar^{q+}$ seeding.

PACS numbers: 34.10.+x

Charge-exchange recombination spectroscopy (CXRS) is a basic tool for accurate evaluation of impurity ion densities in tokamak plasmas. A neutral D or H beam is injected into the plasma and the radiative decay of the excited states formed by electron capture from neutral atoms of the beam by impurity ions is analyzed. It has been recently observed (Isler 1994, Lisse 1997) that energy and/or particle confinement is greatly improved by seeding very highly charged impurities, such $Ne^{q+}$ and $Ar^{q+}$, in the plasma edge. Argon is an important species for ITER (International Tokamak Experimental Reactor) and is acquiring increasing importance in existing tokamak devices. Therefore, accurate partial cross sections for the charge transfer processes involving $Ar^{q+}$ ions are needed in order to check the absolute consistency of CXRS prediction by multiple line observation for the same ions.

The aim of this Letter is to present total and partial $(n, l)$ cross sections for the capture and ionization processes in $Ar^{18+}$ + H(1s) collisions in the energy range of 30 - 300 keV/amu. To our knowledge, this system has never been considered experimentally. Previous Classical Trajectory Monte Carlo (CTMC) calculations (Olson 1981, Pérez *et al* 2001) reported partial cross sections into $n = 8 - 12$ shells of $Ar^{17+}$ for 1 eV/amu $\leq E \leq$100 keV/amu. While these works are well suited to the analysis of x-ray emissions from comets (Cravens 2002, Beiersdorfer *et al* 2003), they are not so useful to the visible emission line measurements that will be undertaken, e.g., at ASDEX-U (Axially Symmetric Divertor Experiment), since these measurements rely on the radiative decay subsequent to charge transfer processes into high-lying states ($n = 14-17$) of the projectile; in particular, for ArXVIII, the relevant transitions are $n$=14-13 ($\lambda$=3448.92 Å), $n$=15-14 ($\lambda$=4275.23 Å), $n$=16-15 ($\lambda$=5223.87 Å) and $n$=17-16 ($\lambda$=6303.27 Å). Whyte *et al* (1998) reported CTMC partial cross sections for $E = 37.5$ keV/amu, and Hung *et al* (http://www-cfadc.phy.ornl.gov/eprints/argon.html ) have performed CTMC calculations for $Ar^{q+}$ + H collisions, with $q = 15-18$, tabulating $n$-, $n, l$-resolved capture cross sections up to $n = 25$, thus encompassing the range of interest for fusion research. Nevertheless, they have used a single-microcanonical distribution to represent the initial H(1$s$) state, and we shall see that this results in inaccurate high-$n$ partial cross sections from low to intermediate impact energies. Here we report improved CTMC calculations whose reliability has been checked, whenever possible, by direct comparison with semi-classical molecular results. Further, as Ar ions progressively strip as they approach the inner plasma region, we also report in this Letter total and partial cross sections for dressed $Ar^{17+}$ and $Ar^{16+}$ ions in collision with H(1$s$).

We do not include here either a description of the method employed, or a discussion of the mechanisms. These details, together with an explanation of the limits of validity of our techniques, can be found elsewhere (Errea *et al* 2004a, Errea *et al* 2004b) for $Ne^{10+}$ + H collisions. As in that work, our calculation employs the impact parameter CTMC formalism (Bransden and McDowell 1992, Illescas *et al* 1998), in which the internuclear vector $\mathbf{R}$ follows linear trajectories $\mathbf{R}$=$\mathbf{b}$ + $\mathbf{v}t$, with impact parameter $\mathbf{b}$ and velocity $\mathbf{v}$, while the electronic initial distribution of the H(1$s$) is obtained from a superposition of ten microcanonical distributions (Hardie and Olson 1983, Illescas and Riera 1999, Errea *et al* 2004b) (henceforward called hydrogenic distribution). Our statistics involve $N$=$10^5$ electronic trajectories for each nuclear trajectory. The Hamilton equations, which describe the electronic motion, were integrated up to time $t_{max} = 500v^{-1}$ au and exit ionizing and capture trajectories were selected by means of the usual energy criterion. The classical phase space of the capture electrons was partitioned into exclusive subspaces, each of them being associated to a quantum state with a definite $n$ and $l$ (Becker and MacKellar 1984). The convergence of the cross sections with respect to increasing values of $N$ and $t_{max}$ has been checked. In the case of the dressed projectiles such $Ar^{16+}$ and $Ar^{17+}$, we have employed Coulomb potentials with effective charges $Z_{eff} = \sqrt{2n_o^2 I}$, where $n_o$ is the principal quantum number of the highest occupied orbital, and I=33.73687 au and 151.43788 au are the experimental ionization potentials of $Ar^{15+}$ and $Ar^{16+}$, respectively (Kelly 1982). For $Ar^{18+}$+H(1$s$) collisions, we performed parallel molecular close-coupling calculations (Errea *et al* 1994) as an indication of the validity of the classical method in the low impact velocity range. The molecular basis included 271 OEDM (One-Electron Diatomic Molecule) orbitals (Power 1973), all $\sigma$, $\pi$ and $\delta$ states that dissociate into $Ar^{17+}(n, l)$+$H^+$ with $n = 7-15$.

Figure (1a) displays the electron loss (i.e., capture + ionization) cross sections obtained by means of the molecular and classical treatments. Regarding the latter,

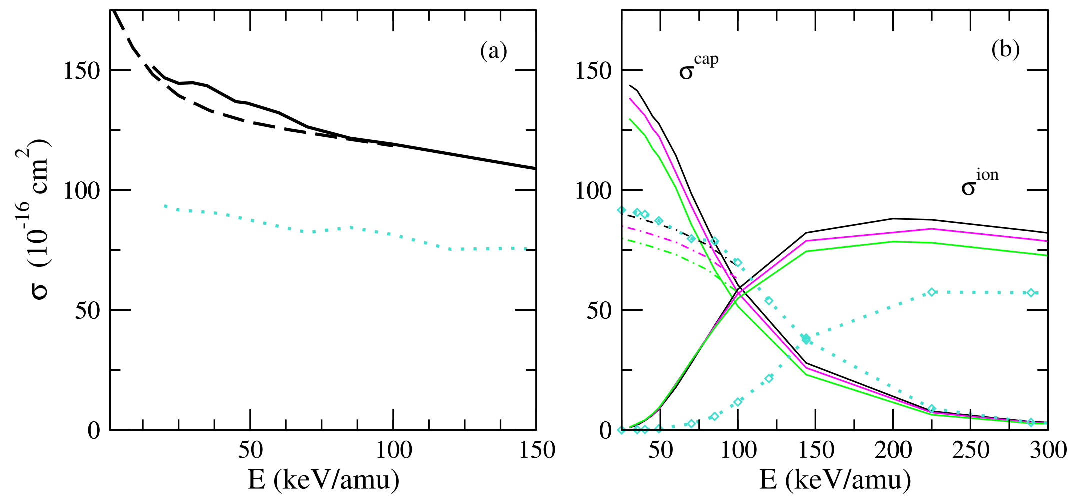


**Figure 1.** Total electron-loss, capture and ionization cross sections in $Ar^{q+}$+H(1$s$) collisions as functions of the impact energy $E$ (keV/amu). (1a) $Ar^{18+}$+H(1$s$) collisions: molecular electron loss (— — —); present classical electron loss: hydrogenic (——) and microcanonical (· · · · ·) results; (1b) hydrogenic CTMC cross sections for $Ar^{18+}$ (——), $Ar^{17+}$ (——), and $Ar^{16+}$ (——) projectiles; three-body single-microcanonical CTMC results from reference (http://www-cfadc.phy.ornl.gov/eprints/argon.html ) (− · −) (same colors for the same collision systems); present single-microcanonical results for $Ar^{18+}$ + H collisions (· · ◇ · ·).

it is clear from this figure that the use of a hydrogenic distribution leads to a cross section that agrees better with the molecular results than the single-microcanonical cross section does. This behaviour holds for all projectile charges, and stems from the ability of the hydrogenic distribution to reproduce the outer part of the initial electronic cloud (Illescas *et al* 1998, Errea *et al* 2004b). The total capture and ionization cross sections for $Ar^{18+,17+,16+}$ + H(1$s$) collisions are detailed in Figure (1b). We have included in this figure results of our hydrogenic calculations, three-body single-microcanonical CTMC results from Hung *et al* (http://www-cfadc.phy.ornl.gov/eprints/argon.html ), as well as our single-microcanonical calculation for $Ar^{18+}$+H collisions. Incidentally, we note the excellent agreement between the three-body and impact-parameter results (within statistical deviations). On the other hand, the use of the single-microcanonical distribution yields a significant underestimation of the total capture cross section for $E \leq 100$ keV/amu as well as of the ionization cross section over the whole impact energy range.

We have checked whether our calculated total cross sections fulfil the scaling relations proposed by Illescas and Riera (1999). For electron capture, we find that our computed cross sections obey the prescribed scaling rule $\sigma_{cap}^{scaled}(q, v') = \sigma_{cap}(2, v)(q/2)^{1.15}$, where $\sigma_{cap}(2, v)$ refers to the $He^{2+}$+H(1$s$) total cross section tabulated in (Illescas and Riera 1999), $v' = v(q/2)^{0.175}$, and $v$ is the impact velocity. Indeed, the largest differences between the computed cross sections and the scaled ones are about 7-9% and in the low-energy region. Similarly, for the total ionization cross sections, the

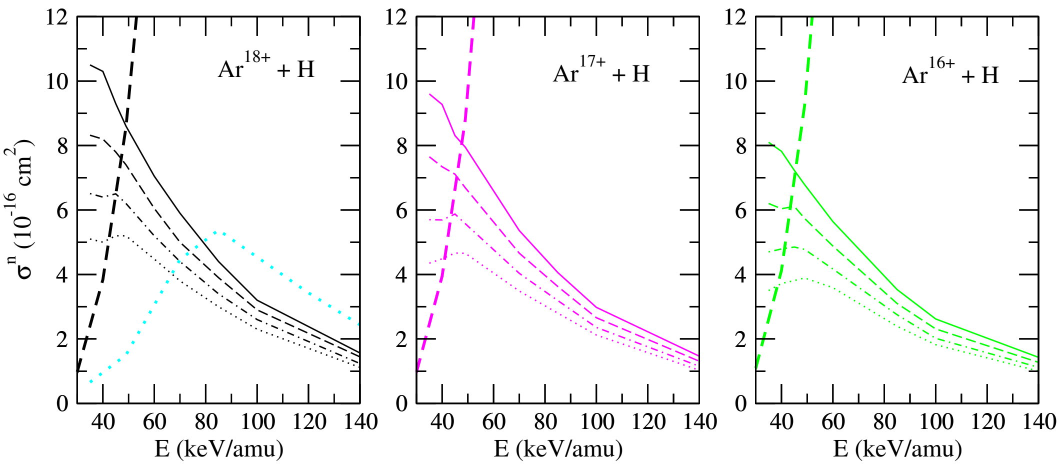


**Figure 2.** $\sigma^n$: $n$-partial cross sections as functions of the impact energy for $Ar^{18+}$ (left), $Ar^{17+}$ (middle), $Ar^{16+}$ (right) + H(1$s$) collisions: (——) n=14, (– – –) n=15, (– · –) n=16 and (· · · · ·) n=17. Our microcanonical CTMC results (· · · · ·) are included in the case of $Ar^{18+}$ + H(1$s$) collisions for $n = 14$. Ionization cross sections (– – –) are also plotted.

simple scaling $\sigma_{ion}^{scaled}(q,v) = \sigma_{ion}(1,v)q^{2[1-exp(-1.4(v-0.76-0.04q))]}$ remains quite good for the present high-$q$ values, although the differences between computed and scaled cross section are larger than for capture (20-25%) and appear at the maximum of the cross section. This behavior can be explained by the fact that the ionization scaling rule was developed for not-too-highly charged projectiles: as we increase $q$ the maximum of the ionization cross section is shifted to lower velocities and becomes broader; as thoroughly studied in Illescas *et al* (1998) and Illescas and Riera (1999), we find that no simple overall scaling rule exists for the ionization probabilities at low $v$ because each of the mechanisms (saddle-point mechanism (Olson 1983, Illescas *et al* 1998), hard encounters with nuclei) that are at work in this velocity regime vary with $v$, $b$, and $q$ in a different way. Finally, at high energies, our calculated ionization cross sections fulfil the $q^2$ first-Born behaviour.

In Figure 2 we present some $n$-partial hydrogenic CTMC cross sections, $\sigma^n(E)$ for $Ar^{18+,17+,16+}$ + H(1$s$) collisions. Our illustration focuses on capture to these very high-lying states of the projectile, with $n = 14 - 17$, which trigger the visible radiative decay that will be analyzed in the future ASDEX diagnostic experiments. Moreover, the impact energy range of Figure 2, $30 \le E \le 140$ keV/amu, overlaps the experimental H beam conditions. This energy range corresponds to the so-called intermediate domain where ionization and charge exchange are competing processes (see Figure 2), and where the semi-classical methods face essential difficulties in providing reliable cross sections. Even our large-scale molecular basis would have to be further enlarged in order to yield converged cross sections for such high-lying (and lowly populated) states. However, such a large effort would seem to be pointless, since improved CTMC calculations have been shown to be especially adequate to the evaluation of high-$n$ cross sections

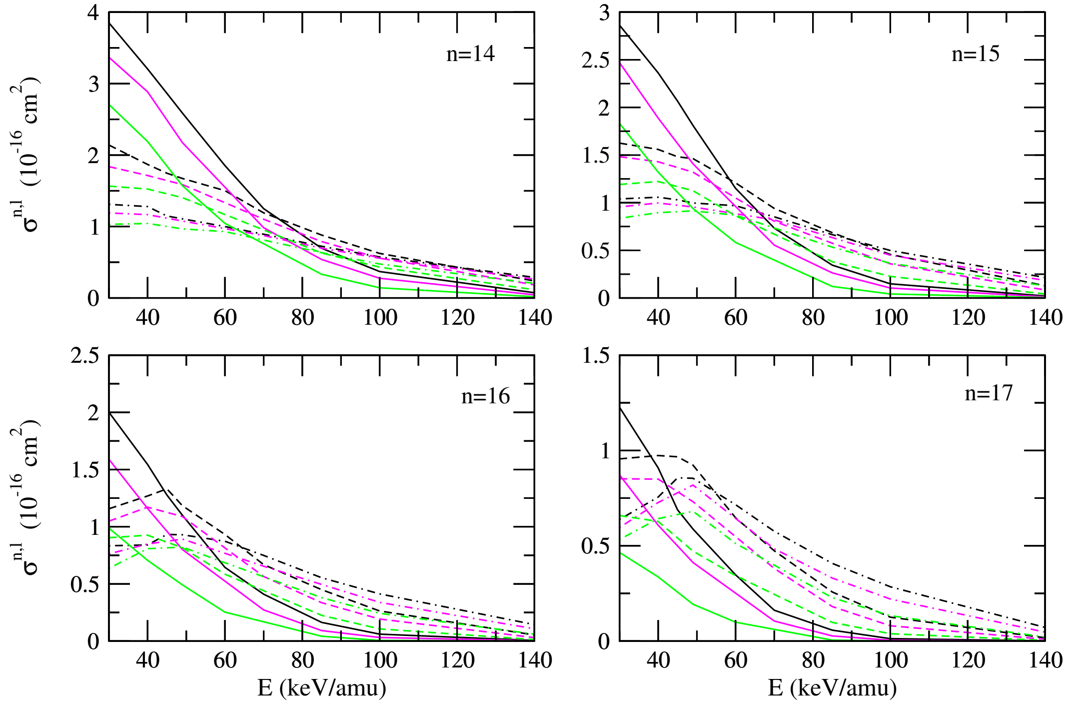


**Figure 3.** $\sigma^{n,l}$: state selective charge exchange cross sections for $Ar^{18+}$ (black), $Ar^{17+}$ (magenta), $Ar^{16+}$ (green) + H(1$s$) collisions as functions of the impact energy. We have plotted (——) $\sigma^{n,n-1}$, (− − −) $\sigma^{n,n-2}$ and (− · −) $\sigma^{n,n-3}$, which are the largest cross sections for these $n$-states.

in the intermediate energy regime (see, e.g., Errea *et al* (2004b)). All the following illustrations, which concern capture processes into very excited states, will thus be restricted to hydrogenic CTMC results. Figure 2 shows similar shapes of the $n$-partial cross sections for $q$ ranging from 16 to 18. The Oppenheimer $n^{-3}$ rule (Oppenheimer 1928) holds for $E \geq 70$ keV/amu and $n \geq 16 - 18$ for the three systems, and can be employed to extrapolate our data for $n > 17$. We further illustrate in Figure 2, in the case of $Ar^{18+}$+H(1$s$) collisions, the large underestimation when using a single-microcanonical distribution, from low to intermediate-$E$, of the high-$n$ capture cross sections. On the other hand, the microcanonical and hydrogenic results coalesce in the high impact energy range (see, e.g., Fig. 1b), where the capture process takes place through sudden momentum transfer from the target to the projectile, and this process is similarly described by means of the two initial distributions. As already pointed out, the $n = 14 - 17$ levels are lowly populated, and the main outputs of capture consist of the levels $n_{max} = 9 - 10$ (for $q = 16 - 18$). For these dominant channels, the single-microcanonical CTMC results turn out to be more accurate than the hydrogenic ones in the intermediate energy region, as explained in Errea *et al* (2004b).

In Figure 3 we present $(n, l)$-partial cross sections, $\sigma^{nl}(E)$, with $n = 14 - 17$, for $Ar^{18+,17+,16+}$ + H(1$s$) collisions and $30 \leq E \leq 140$ keV/amu. As capture to these high-$n$ shells mainly produce captured orbits characterized by large $l$ values, we have plotted,

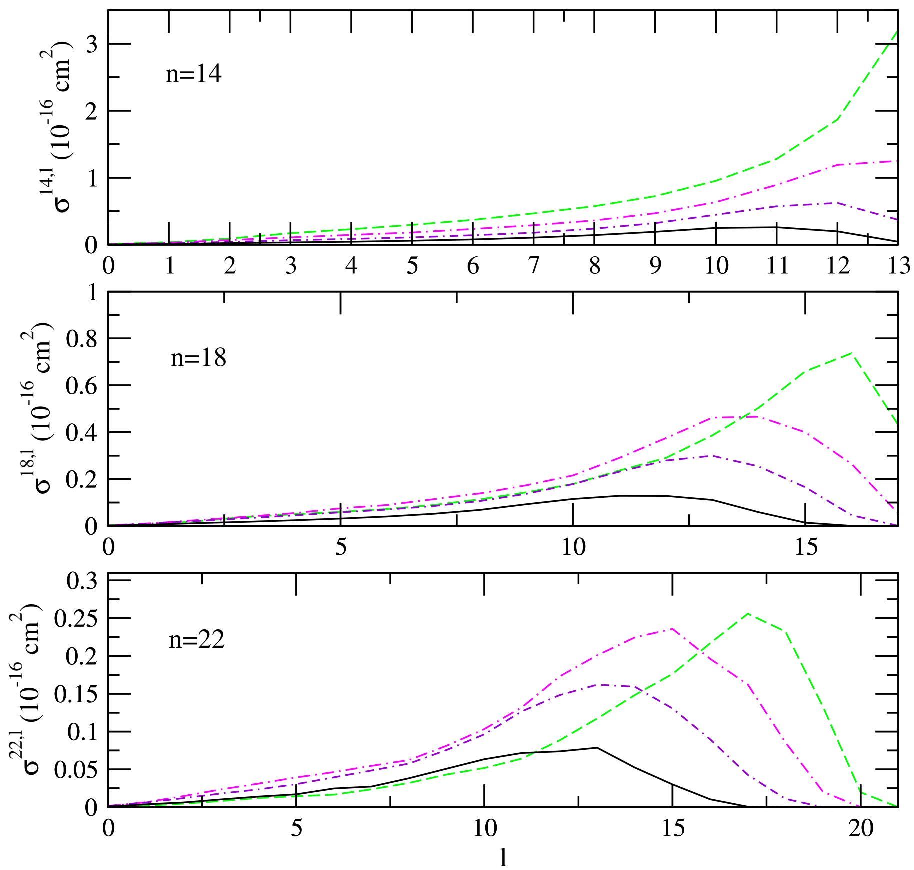


**Figure 4.** $\sigma^{n,l}$: $l$-distributions in $Ar^{18+}$ + H(1$s$) collisions for selected final quantum states: $n = 14$ (top), $n = 18$ (middle) and $n = 22$ (bottom) and selected collision energies: $E = 40$ (— — —), 70 (– · –), 100 (· – –·), and 144 keV/amu (——).

for the sake of clarity, the (largest) cross sections associated to the specific subshells with $l = n-1, n-2$ and $n-3$. For all ion charges and $n$ considered, $l = n-1$ is the main contribution to the $n$-shell population at the lowest impact energy $E \sim 30$ keV/amu. As the impact energy increases, this contribution drops quite rapidly so that $l = n-2$ becomes the more probable angular momentum within the shell. For further high $E$, $l = n-2$ population vanishes and $l = n-3$ is the leading subshell. The relay towards lower $l$ ends up at E $\sim$ 300 keV/amu with a maximum population for $l \sim 9$, and would terminate at very high energies with $l = 0$ maximum contribution, as predicted by perturbative treatments (see, e.g., Belkič *et al* (1992)).

As we have not found significant differences in the behaviour of the $(n, l)$-state selective capture cross sections for the three collision systems considered here, we have chosen the stripped ion collision, $Ar^{18+}$ + H(1$s$), to illustrate in detail the $l$-distributions to the partial $n$-cross sections; these are displayed in Figure 4 for $E$ ranging from 40 to 144 keV/amu, and for three typical $n$-shells that respectively comply with $n < q$ ($n = 14$), $n = q = 18$ and $n > q$ ($n = 22$). It is clear that as $E$ increases the downward shift of the maximum $l$-contribution to a given $\sigma^n$ cross section appears the sooner the larger is $n$. Furthermore, in the cases of very high-lying shells ($n > q$), the $\sigma^{n,l}/\sigma^{n}$ ratio is never found to display a maximum for $l = n - 1$ at the threshold of the intermediate impact energy range; a bounding value of $l \sim 17$ is rather observed.

To sum up, the aim of this work is to propose accurate cross sections for $Ar^{q+}$ + H(1$s$) collisions, to be used in fusion research. From previous work showing the significant improvement of the ionization, total capture and high-lying partial capture cross sections reached by using a hydrogenic initial distribution in a CTMC context (Illescas and Riera 1999, Errea *et al* 2004b), we have presented new results for capture to high $(n, l)$ levels in $Ar^{q+}$ + H(1$s$) collisions, which are crucial to diagnostics of plasmas involving Ar seeding.

## Acknowledgments

This work has been partially suportted by DGICYT projects ENE2004-06266 and FIS2004-04145, and the Acción Integrada Hispano Francesa AIHF 2003-0171.

## References

Abrines R and Percival I C 1966 *Proc. Phys. Soc.* **88** 861

Becker R L and MacKellar A D 1984 *J. Phys. B: At. Mol. Phys.* **17** 3923

Beiersdorfer P, Boyce K R, Brown G V, Chen H, Khan S M, Kelley R L, May M, Olson R E, Porter F S, Stahle C K and Tillotson W A 2003 *Science* **300** 1558

Belkič D, Gayet R and Salin A 1992 *At. Data Nucl. Data Tables* **51** 76

Bransden B H and McDowell M. H C 1992 *Charge Exchange and the Theory of Ion-Atom Collisions* Oxford, Clarendon

Cravens T E, 2002 *Science* **296** 1042

Errea L F, Harel C, Jouin H, Méndez L, Pons B and Riera A 1994 *J. Phys. B: At. Mol. Phys.* **27** 3603

Errea L F, Illescas C, Méndez L, Pons B, Riera A and Suárez J 2004*a J. Phys. B: At. Mol. Phys.* **37** 4323

Errea L F, Illescas C, Méndez L, Pons B, Riera A and Suárez J 2004*b Phys. Rev. A* **70** 052713

Hardie D J W and Olson R E 1983 *J. Phys. B: At. Mol. Phys.* **16** 1983

Hung C C, Krstic P S and Schultz D R *http://www-cfadc.phy.ornl.gov/eprints/argon.html*

Illescas C, Rabadán I and Riera A 1998 *Phys. Rev. A* **57** 1809

Illescas C and Riera A 1999 *Phys. Rev. A* **60** 4546

Isler R C 1994 *Plasma Phys. Control Fusion* **36** 171

Kelly R L 1982 *Atomic and ionic spectrum lines below 2000 Å* Oak Ridge National Laboratory

Lisse C M 1997 *Science* **277** 1625

Olson R E, 1981 *Phys. Rev. A* **24** 1726

Olson R E, 1983 *Phys. Rev. A* **27** 1871

Oppenheimer J R 1928 *Phys. Rev.* **31** 349

Pérez J A, Olson R E and Beiersdorfer P 2001 *J. Phys. B: At. Mol. Phys.* **34** 3063

Power J D 1973 *Phil. Soc. Trans. R. Soc.* **274** 663

Summers H P, Badnell N D, O'Mullane M G, Whiteford A D, Bingham R, Kellett B J, Lang J, Behringer K H, Fantz U, Zastrow K-D, Loch S D, Pindzola M D, Griffin D C and Ballance C P 2002 *Plasma Phys. Control. Fusion* **44** B323

Whyte D G, Isler R C, Wade M R, Schultz D R, Krstic P S, Hung C C and West W P 1998 *Physics of Plasmas* **5** 3694